

Monitoring of stress distribution in damaged small-scale masonry walls by using two innovative sensors

Original

Monitoring of stress distribution in damaged small-scale masonry walls by using two innovative sensors / Concetta Oddo, Maria; Camarda, Gaetano; Minafò, Giovanni; Fabio Granata, Michele; Bertagnoli, Gabriele; DI TRAPANI, Fabio; Pennisi, Agatino; Barile, Simone. - In: PROCEDIA STRUCTURAL INTEGRITY. - ISSN 2452-3216. - ELETTRONICO. - 44:(2023), pp. 798-805. (Intervento presentato al convegno ANIDIS XIX & ASSISi XVII - 2022 tenutosi a Torino nel 11 settembre 2022 – 15 settembre 2022) [10.1016/j.prostr.2023.01.104].

Availability:

This version is available at: 11583/2978622 since: 2023-06-04T01:24:21Z

Publisher:

Elsevier

Published

DOI:10.1016/j.prostr.2023.01.104

Terms of use:

openAccess

This article is made available under terms and conditions as specified in the corresponding bibliographic description in the repository

Publisher copyright

(Article begins on next page)

XIX ANIDIS Conference, Seismic Engineering in Italy

Monitoring of stress distribution in damaged small-scale masonry walls by using two innovative sensors

Maria Concetta Oddo^{a,*}, Gaetano Camarda^a, Giovanni Minafò^a, Michele Fabio Granata^a, Gabriele Bertagnoli^b, Fabio Di Trapani^b, Agatino Pennisi^c, Simone Barile^d

^a*Dipartimento di Ingegneria, Università degli Studi di Palermo, Palermo, Italy*

^b*Dipartimento di Ingegneria Strutturale, Edile e Geotecnica, Politecnico di Torino, 10129, Turin, Italy*

^c*STMicronics S.r.l., System Research and Application, Catania, Italy*

^d*MAPEI Spa, Milan, Italy*

Abstract

Structural Health Monitoring (SHM) represents a strategic solution for the preservation of cultural heritage buildings. Existing masonry structures often suffer reductions in mechanical performances due to physiological aging of material constituents, external actions, and effect of catastrophic natural events. In many cases, the prompt prediction of damage in masonry elements is difficult and it can cause sudden collapses, compromising the safety of people.

The proposed experimental study examines the effectiveness of two low-cost and innovative stress sensors, i.e. piezoelectric and capacitive stress sensors, for SHM of masonry structures. To this scope, the sensors were embedded in the mortar joints of two small-scale clay brick and calcarenite masonry wall specimens consisting of three panels. Experimental tests were carried out by applying a constant vertical compressive load at the top of each specimen and simulating the damage with a progressive reduction of the cross-section of one of the panels. During the tests, the vertical stress distributions (and their variations), were monitored by the sensors. Experimental outcomes from sensor reading were then compared to that numerically provided by a refined finite element simulation of the test. Results will show that vertical stress variations in masonry structures can be effectively accounted by the adopted sensors and potentially interpreted for the early prediction of structural damage.

© 2023 The Authors. Published by Elsevier B.V.

This is an open access article under the CC BY-NC-ND license (<https://creativecommons.org/licenses/by-nc-nd/4.0>)

Peer-review under responsibility of the scientific committee of the XIX ANIDIS Conference, Seismic Engineering in Italy.

Keywords: Type your keywords here, separated by semicolons ;

1. Introduction

In recent years, the huge growth of the capabilities of smart sensing technology and artificial intelligence, has attracted the scientific community towards the assessment of near-real-time performance of civil structures and infrastructures (Sohn et al. 2003, Balageas et al. 2010, Farrar and Worden 2012, Sony et al. 2019). Special attention has been addressed to the existing built heritage, firstly because of the natural aging process and deterioration of materials, which undermines the structural safety under service and extraordinary loads. The need for a permanent monitoring system, able to provide useful real-time information to control the current safety levels and service conditions over the time, led to the development of new generations of low-cost sensors both for static and dynamic monitoring. During the last decade, the development of high-speed internet and the birth of cloud-based services and big data platforms, where artificial intelligence algorithms can be applied for data processing, have enhanced the capability of structural health monitoring.

As regards sensors, special attention has been paid to new-generation low-cost sensors, based on Micro Electro-Mechanical Systems (MEMS) technology. These sensors recognize micro-movements of micrometric mechanical systems. MEMS include inclinometers, accelerometers and magnetometers. Besides MEMS technology, new stress sensors based on piezoresistive or capacitive technologies delineate an emerging category of monitoring devices. Piezoresistive stress sensors with ceramic sensing package have been already used embedded in concrete structures, while capacitive stress sensors are available only as prototypes and are still under test. Both the sensors are thought to be used in new and existing structures although with different modalities of installation. The potential use of piezoresistive and capacitive stress sensors for SHM of masonry structures has been also recently tested at the Material and Structures Test Laboratory of the University of Palermo (La Mendola et al. 2021a). In this case sensors were embedded within the mortar bed-joints of 12 masonry wall specimens subject to compression. Results have shown a good capability of pre-installed piezoresistive ceramic and capacitive sensors to capture the vertical stress variation in the masonry as a consequence of the external loads directly applied on the specimens, while their performance in the post-installed configuration is ongoing in a separate investigation.

In the framework of real-time SHM of masonry structures, embedded sensors are thought to be used to predict potential structural damage as a consequence of the modification of the internal stress state, and so to provide early warnings. Information from the embedded sensors could be also fundamental to the definition of digital twins of masonry structures, as already occurs for civil infrastructures (Hua-Peng et al. 2018, Sheng et al. 2022).

On the other hand, it should be said that the actual stress distribution in real masonry structures is much more complex than the one occurring on the single masonry wall panel, where these sensors have been tested. In this context, the capability of the embedded sensors to be able to provide reliable and useful information to SHM of masonry structures deserves additional investigation. To this aim, this paper presents an extension of the experimental study carried out by La Mendola et al. (2021a), to an entire half-scale masonry wall composed of three panels. The tests consisted of the application of a constant vertical load at the top of the specimen. Then the damage was introduced in the central wall panel by a progressive reduction of its cross-section. Piezoelectric and capacitive sensors installed within the mortar joints were used to record the vertical stresses and their variation during the tests. Stress values recorded by the specimens were then compared to that of a refined finite element (FE) micro-model realized in **Abaqus**® simulating the experimental tests. Comparison between recorded stresses and numerically obtained ones showed a certain consistency especially for what concerns the capability of the sensors to recognized even slight stress variations. The tests also regarded the same sensors in the post-installed configuration. However, results from this last application are still under processing.

2. Resume on the proposed piezoresistive ceramic and capacitive sensors

Piezoresistive ceramic sensors include electronic circuits, which are based on a microcontroller with embedded memory flash (Fig. 1a). The latter can read the low electrical signal of piezoresistive bridges and convert it into a digital value. Since ceramic is a perfectly elastic material, a direct calculation of the stress in a given direction is possible in the field of the elastic service stresses without any direct measure of deformation. The sensor was initially designed to be embedded inside concrete casting tied to the rebars (Bertagnoli 2016, Abbasi et al., 2017, Anerdi et al. 2020, Abbasi et al. 2021).

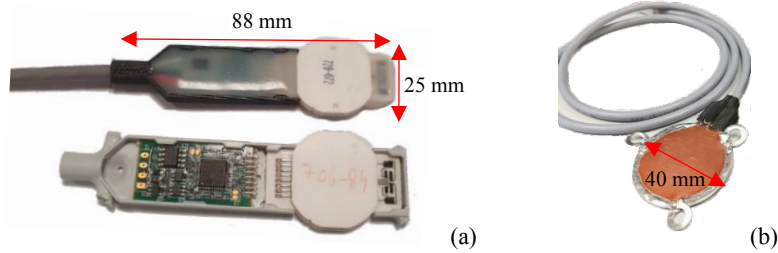


Fig. 1. (a) Piezoresistive ceramic sensors; (b) Capacitive sensors. (Figures from La Mendola et. al. 2021b)

The capacitive sensor (Fig. 1b) consists of a parallel-plate capacitor with Kapton as a dielectric layer. The sensing area is a planar circular surface with a diameter of 40 mm. The capacitance, C , of a parallel plate capacitor is given by the following expression:

$$C = \frac{\varepsilon A}{d} \quad (1)$$

where ε , A and d are the permittivity of the gap, the area of electrodes, and the gap between the electrodes, respectively. The variation of the capacitance is related to the deformation according to the variation of the distance between the electrode plates. The sensor reader is a signal conditioning electronics which converts the capacitance signal to voltage, current or frequency. The reader used for capacitive sensors makes use of a microcontroller and it is located outside the sensing part. Capacitive sensors offer different advantages including high sensitivity, high stability, low temperature sensitivity, low production costs and durability. Even these kinds of sensors have been originally designed to be placed within concrete members (Pappalardo et al. 2019).

The potential use of both piezoelectric and capacitive sensors to monitor normal stresses of masonry structures have been also recently tested (La Mendola et al. 2021a) by imbedding them inside mortar bed-joints (Fig. 2). Results have shown that both the sensors were effectively sensitive to the vertical stress variations in the pre-installed configuration.

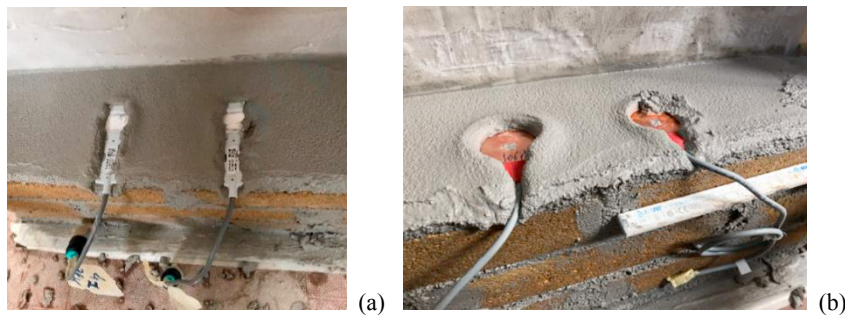


Fig. 2. Installation of the sensors in the mortar bed-joints: (a) ceramic sensors; (b) capacitive sensors. (Figures from La Mendola et. al. 2021b)

3. Specimen details and testing modalities

The tests were carried out at the Material and Structures Test Laboratory of the University of Palermo. The specimens consisted of two half-scale masonry walls, one made of clay bricks, one of calcarenite bricks. The typical arrangement of the specimens is illustrated in Fig. 3a. The overall dimensions of a specimen are 2285 x 1250 mm. Two window-openings of 387 x 430 mm are provided in the wall, so that three wall-panels of 500 x 430 mm are formed. The bricks had standard size of 250 x 120 x 50 mm and were arranged with a M5 grade mortar ($f_{mm}=8.36$ MPa). The mechanical characterization of the bricks and of the masonry walls has been previously carried (La Mendola et al. (2021b)). The average compressive strengths of the bricks were 11.80 MPa and 23.39 MPa for

calcarenite and clay bricks, respectively. As regards masonry, average compressive strengths were 7.36 MPa and 13.91 MPa for calcarenite and clay, respectively.

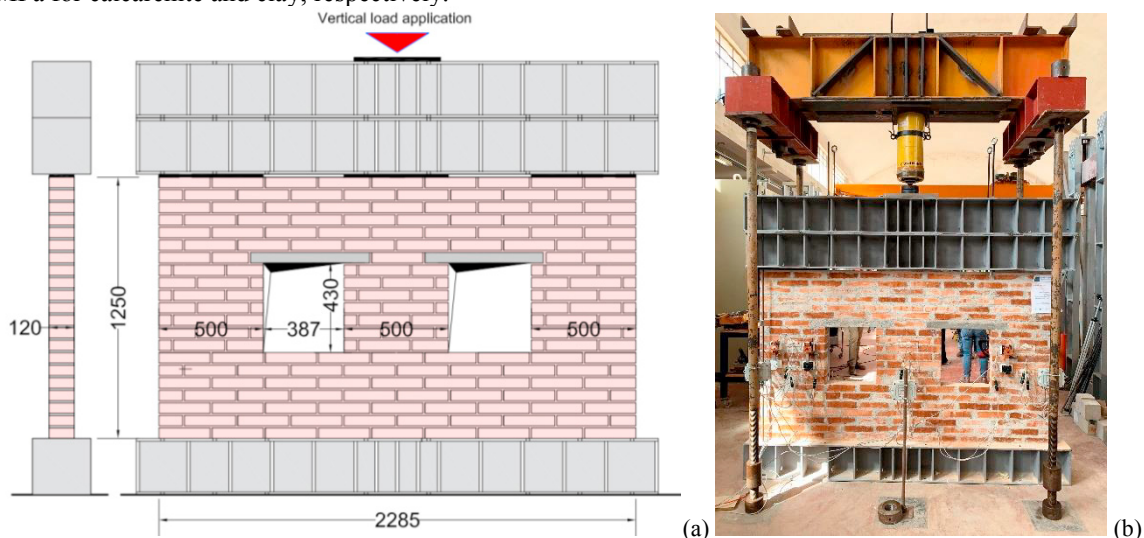


Fig. 3. (a) Design details of a specimen; (b) Test setup picture for the clay brick masonry specimen.

The test setup and the instrumentation are shown in Fig. 3b. The test consisted in the application of a reference service load from the top of the specimen by means of a hydraulic jack. The service load was 500 kN for the clay brick walls and 300 kN for the calcarenite walls. A stiff steel beam was used to transfer approximately the same rate of vertical load to the three wall panels. The steel beam was leaning on three steel plates having the same dimensions of the wall panels. This allowed centering the vertical load acting on each wall panel. The test was performed in two steps. First the vertical load was applied to simulate a service load condition for a masonry wall subject to gravity loads. In the second step the collapse of the central panel is simulated by performing a progressive reduction of the cross section up to the complete removal of the panel. The cross-section reduction was performed in three steps: from 50 to 40 cm (Fig. 4a), from 40 to 15 cm (Fig. 4b) and finally the complete removal of the central wall panel (Fig. 4c).

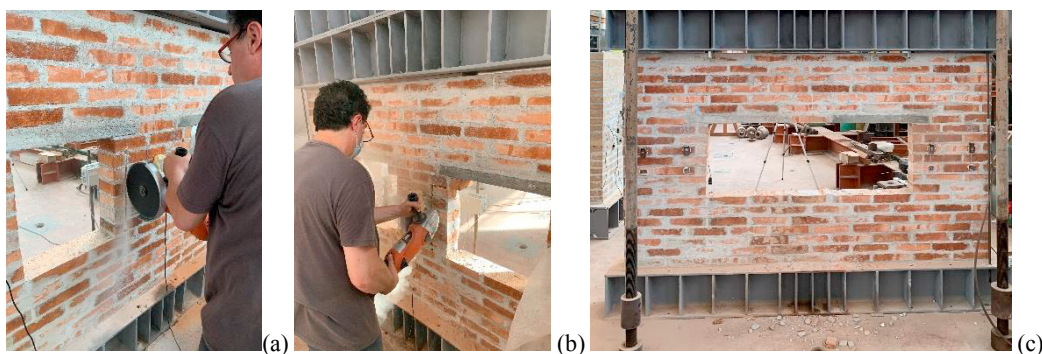


Fig. 4. Damage simulation in the central wall: (a) first cross-section reduction; (b) second cross-section reduction; (c) central wall removal.

During the progressive reduction of the cross section, the vertical load was kept constant, and the vertical stress redistribution was recorded by the sensors embedded in the three wall panels named M1, M2 and M3 (Fig. 5a). Two sets of pre-installed sensors were arranged (Fig. 5a), one set for the piezoresistive ceramic sensors, the other for the capacitive sensors. Each set consisted of 7 sensors. For the central panel, only one sensor per typology is placed in correspondence of the mid-height cross-section along the central alignment (Fig. 5b). Sensors installed on M2 wall panel could provide stress measures up to the damage step before the complete removal of the wall since they were removed in the last step. For the external panels (M1 and M3), the sensors were placed in correspondence of the

central alignment of the panel and in correspondence of the inner and outer sides of the wall.

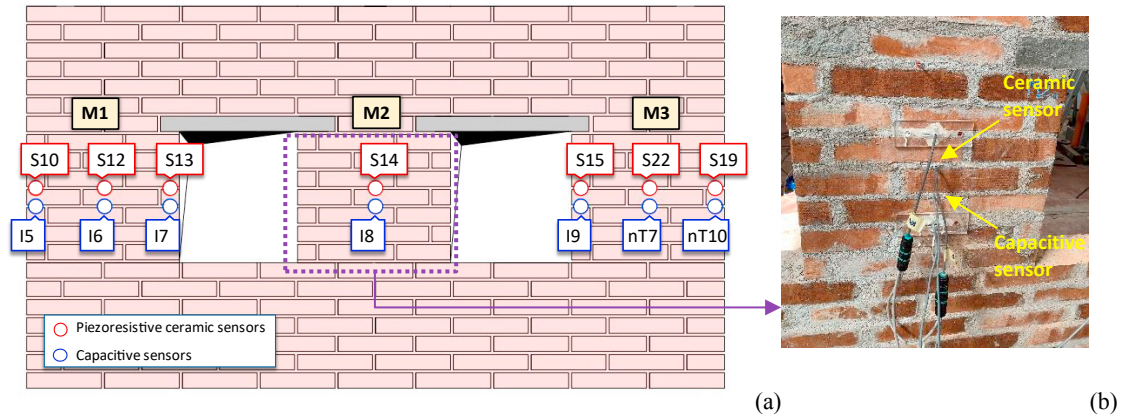


Fig. 5. (a) Sensor placement layout; (b) View of a masonry panel with the embedded sensors.

This configuration of the sensors was chosen to measure the vertical stresses at the centroid and at the extremal points of a wall panel cross-section, in such a way to recognize the expected increase of flexural action on the external wall panels due to the stress redistribution caused by the progressively induced damage. Ceramic and capacitive sensor sets were also arranged in the post-installed configuration. Results from these sensors are still under processing and will not be presented in this paper.

4. Numerical simulation of the test

The numerical simulation of the tests was carried out using a refined numerical model realized with the Abaqus® software platform. The model was defined with 3D solid elements for the bricks, the mortar, and the steel elements (Fig 6a). The model was realized as a partitioned continuum body (hard contact) to assign different material properties to the bricks, the mortar and the steel members. As regards bricks and mortars, the concrete damaged plasticity model was used, while steel elements were modelled as elastic. The material models were defined using the average experimental values for the materials strengths reported in Section 3. The load application to the model provided first the application of gravity load, then the application of the external load up to the reference value. The load is then kept constant up to the end of the test (Fig. 6b). In this stage, the cross-section reduction is simulated as a staged construction (model change function) by removing the element portions in the same way as it is done in the real test. For the sake of space, results in the following will be only shown for the clay brick masonry wall specimen.

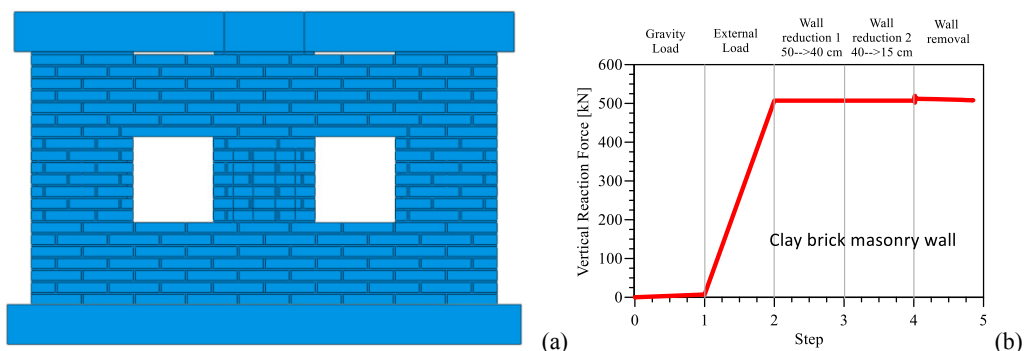


Fig. 6. (a) View of the FE model; (b) Load pattern application to the model.

Vertical stresses were monitored during the simulation of the tests. In particular, 14 measuring points were placed in the model in correspondence of the same points where the pressure sensors were placed. An overall view of the vertical stresses distribution and of their variation during the FE simulation is provided in Fig. 7. As it can be observed, vertical stresses at the first step are approximately uniformly distributed on the three wall panels (Fig. 7a). The progressive reduction of the cross-section of the central wall panel (M2) provides an increase of the compressive stress on it. A further increase of the compressive stresses is recognized on the lateral wall panels because of the progressive load transfer occurring. In particular, a kind of arching response of the system is recognized. The external wall panels undergo a major normal stress increment in proximity of the inner monitoring points, meaning that these panels are subjected to an additional flexural demand.

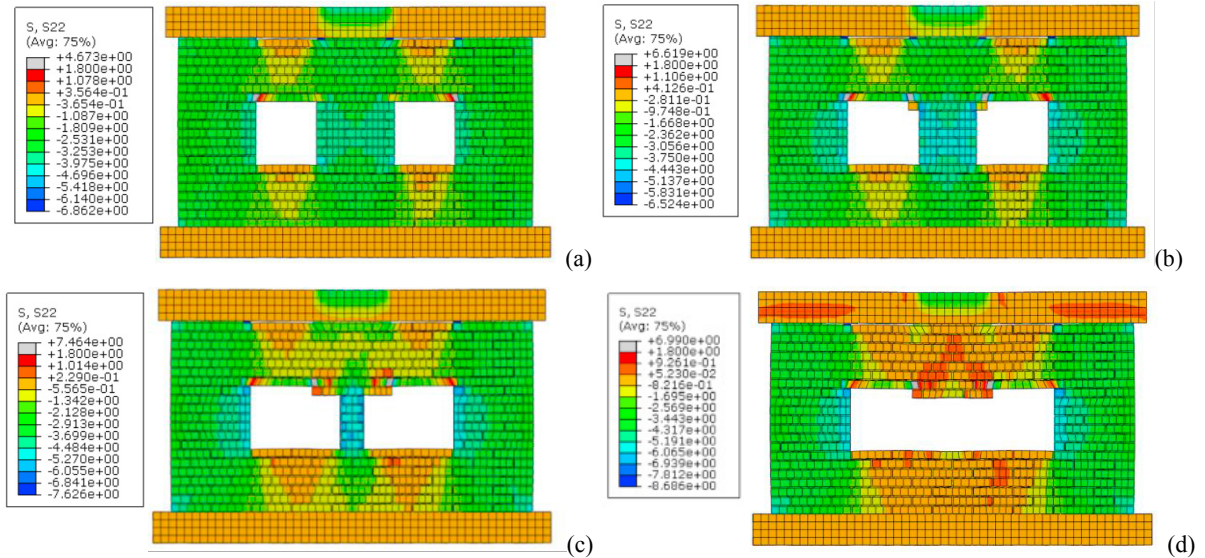


Fig. 7. Vertical stresses during the test simulation: (a) load application; (b) wall reduction 1; (c) wall reduction 2; (d) wall removal.

5. Experimental and numerical test results and comparisons

The stress patterns evaluated for the refined FE model are used as reference for the comparison with the sensor readings. Given that the measuring points of ceramic sensors and of the respective capacitive sensors vertically aligned are really close, a unique stress measure for each alignment is used as reference from the FE model.

5.1. Results from comparisons with piezoresistive ceramic sensors

Results of comparisons between ceramic sensor readings and the reference vertical stresses measured with the FE model are shown in Fig. 8 for all the sensors. It can be observed that the overall trend of sensor recordings reasonably follows the FE obtained results. The different phases of the tests can be clearly distinguished from the sensor readings. The diagrams show an initial increase of the vertical stress up to the value associated with the achievement of the service load. The subsequent vertical stress increases occur because of the central cross-section reduction. Each cross-section cut induces an increment of the slope of the vertical stress diagram, which is generally well captured from the sensors. A good agreement between numerical and experimental results was also found in terms of current stress values in most cases. In particular, the different vertical stress trend on the wall panels well reflects the rapid increase of the compressive stress in the M2 panel due to the reduction of the cross-section (Fig. 8a) and the increment of the flexural demand on the outer panels (Figs. 8a-8c).

5.2. Results from comparisons with capacitive sensors

Capacitive sensors provided capacitance measures. In order to perform a qualitative comparison with the FE model stress recordings, the capacitance readings were normalized in the same way as it was done by La Mendola et al. 2021a. In detail, the initial capacitance value (C_0) was subtracted to the current capacitance values (C), so that $\Delta C = C - C_0$. After, ΔC is normalized by the maximum capacitance variation ($\Delta C_{max} = C_{max} - C_0$). In this way the normalized capacitance is $\Delta C / \Delta C_{max} (\leq 1)$. Results of comparisons between capacitive sensor normalized capacitances and the reference vertical stresses measured by the FE model are shown in Fig. 9. In this case, the comparison is only qualitative in a double vertical axes diagram, where the maximum stress from the FE model corresponds to a normalized capacitance of 1. Results for the M2 wall were not reported as the capacitive sensor installed in this panel underwent some damage during the test. Overall, the qualitative comparison results in agreement with the previously recognized trend. The capacitive sensors were able to recognize the stress variations associated with the different steps of the test. It is noteworthy observing that the trend of the normalized capacitance after application of the vertical load follows an approximately linear trend, instead of an exponential one. However, the relationship between capacitance and stress for these sensors is still under investigation.

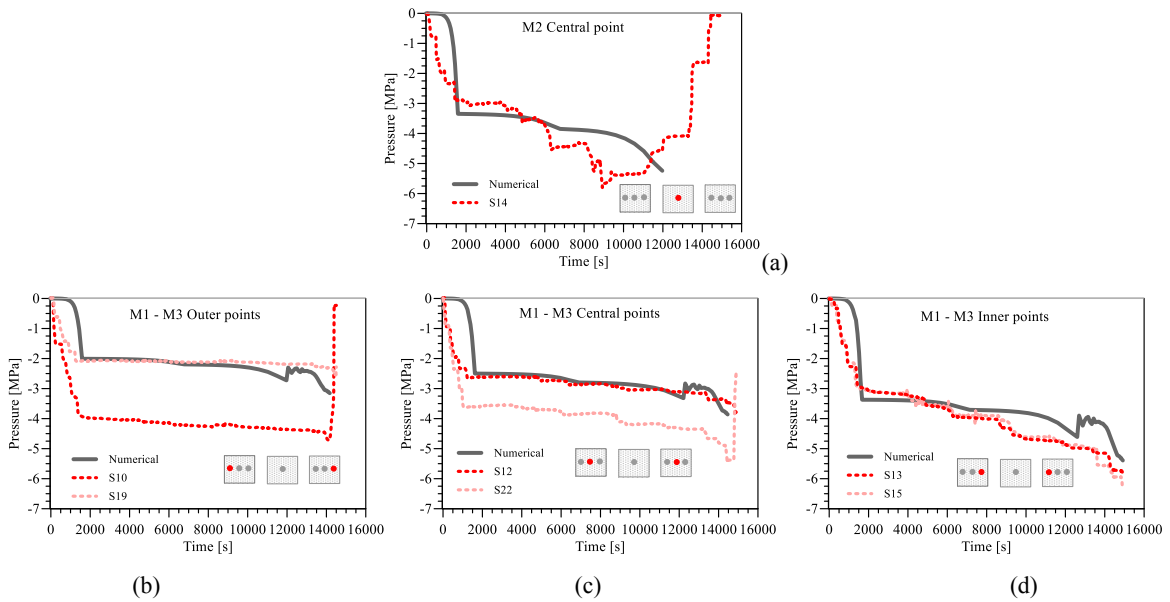


Fig. 8. Comparison between numerically evaluated vertical stresses and vertical stresses recorded by the piezoresistive ceramic sensors: (a) M2 wall; (b) M1-M3 walls at outer points 1; (c) M1-M3 walls at central points; (d) M1-M3 walls at inner points.

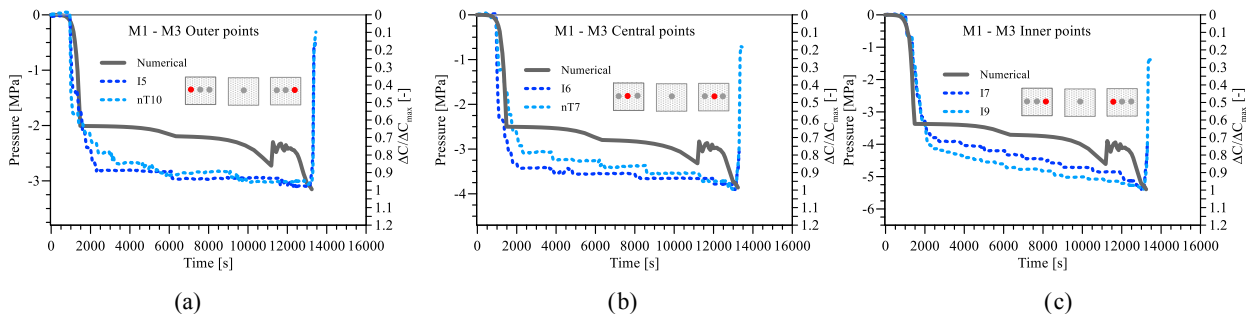


Fig. 9. Comparison between numerically evaluated vertical stresses and normalized capacitances recorded by the capacitive sensors; (a) M1-M3 walls at outer points 1; (b) M1-M3 walls at central points; (c) M1-M3 walls at inner points.

6. Conclusions

The paper presented the results of an experimental campaign on two types of stress sensors, namely piezoresistive ceramic sensors and capacitive sensors, embedded in mortar joints of masonry walls. The sensor performances were tested on a half-scale masonry wall composed of three panels. The tests consisted of the application of a constant vertical load at the top of the specimen and a subsequent progressive reduction of the cross-section of the central wall panel to simulate the damage. Stress values recorded by the sensors placed in the specimen were then compared to that of a refined finite element (FE) micro-model used as reference. Comparisons between sensor readings and results from FE model allowed concluding that both the sensors can effectively capture the overall trend of the stress variations in case of stress redistributions due to unexpected events. Ceramic sensors also allow a good estimation of the current stress acting in the walls. Capacitive sensors have the advantage to have a low cost. Their use is currently limited to the recognition of capacitance variations, which however can be still interpreted in the framework of SHM of masonry structures to predict potential structural damage as a consequence of the modification of the internal stress state, and so to provide early warnings. Results here presented refer to the sensors arranged in the pre-installed configuration. Nevertheless, these preliminary results are fundamental to understand the behaviour of sensors in the post-installed configuration, whose data are currently in the data processing stage.

Acknowledgements

The paper was supported the Industrial Research Project of the Italian Ministry of Research (MIUR) in the field of “Smart Secure & Inclusive Communities PON INSIST – Sistema di Monitoraggio INtelligente per la SICurezza delle infraSTRutture urbane”

References

- ABAQUS. ABAQUS theory and user manuals, version 6.14, 2014.
- Abbasi, M., Anerdi, C., Bertagnoli, G., 2021. An embedded stress measure of concrete: A new sensor able to overcome rheology issues, Proc. Italian Concrete Days 2020, Naples.
- Abbasi, M., Bertagnoli, G., Caltabiano, D., Guidetti, E. (inventors). ST Microelectronics s.r.l. (Assignee). Stress sensor for monitoring the health state of fabricated structures such as constructions, buildings, infrastructures and the like, Patent No. EP 3 392 637 B1, 2017.
- Anerdi, C., Gino, D., Malavisi, M., Bertagnoli, G., 2020. A Sensor for Embedded Stress Measure of Concrete: Testing and Material Heterogeneity Issues. In: di Prisco, M., Menegotto, M. (eds) Proceedings of Italian Concrete Days 2018. ICD 2018. Lecture Notes in Civil Engineering, vol 42, Springer.
- Balageas, D., Fritzen, C.P., Güemes, A., 2010. Structural health monitoring, Vol. 90, Wiley.
- Bertagnoli, G. (inventor). Safecertifiedstructures Tecnologia (Assignee). Method and investigation device for measuring stresses in an agglomerate structure, Patent No. WO2017/178985 A1, 2016.
- Farrar, C.R., Worden, K., 2012. Structural Health Monitoring: A Machine Learning Perspective, John Wiley & Sons.
- Hua-Peng, C., Yi-Qing, N., 2018. Structural Health Monitoring of Large Civil Engineering Structures. John Wiley & Sons Ltd.
- La Mendola, L., Oddo, M.C., Papia, M., Pappalardo, F., Pennisi, A., Bertagnoli, G., Di Trapani, F., Monaco A., Parisi, F., Barile, S., 2021a. Performance of two innovative stress sensors imbedded in mortar joints of new masonry elements. Construction and Building Materials 297, 123764.
- La Mendola, L., Oddo, M.C., Papia, M., Pappalardo, F., Pennisi, A., Bertagnoli, G., Di Trapani, F., Monaco A., Parisi, F., Barile, S., 2021b. Experimental testing of two novel stress sensors for shm of masonry structures. 12th International Conference on Structural Analysis of Historical Constructions SAHC 2020.
- Pappalardo, F., Pennisi, A., Guidetti, E., Doriani, A. (inventors). ST Microelectronics s.r.l. (Assignee) Capacitive pressure sensor for monitoring construction structures, particularly made of concrete, Patent n. US 10,914,647 B2, 2019.
- Sheng, Y., Dongsheng, L., Jinping, O., 2022. Digital twin-based structure health hybrid monitoring and fatigue evaluation of orthotropic steel deck in cable-stayed bridge. Structural control and health monitoring 29(8), e2976.
- Sohn, H., Farrar, C.R., Hemez, F.M., Shunk, D.D., Stinemates, D.W., Nadler, B.R., Czarnecki, J.J., 2003. A Review of Structural Health Monitoring Literature: 1996–2001, Los Alamos National Laboratories.
- Sony, S., Lavature, S., Sadhu, A., 2019. A literature review of next-generation smart sensing technology in structural health monitoring. Struct. Control Health Monitor. 26(3), e2321.